COBEM 2023 27TH INTERNATIONAL CONGRESS OF MECHANICAL ENGINEERING

ABCM Brazilian Society of Mechanical Sciences and Engineering
27th ABCM International Congress of Mechanical Engineering
December 04-08, 2023, Florianópolis-SC, Brazil

COB-2023-1906
NUMERICAL AND EXPERIMENTAL ANALYSIS OF ROTATING BLUNT BODIES TRAJECTORY AT SEA-LEVEL CONDITIONS

Geovanna S. Borges
Olexiy Shynkarenko
Patrick Christian de Melo
Washington Siqueira da Macena
Gibran Cavalcante Alves Silva
Faculdade UnB Gama, Universidade de Brasília, Área Especial de Indústria Projeção A, Setor Leste, Gama, CEP 72.444-240
geovannadalinajara7@gmail.com
olexiy@aerospace.unb.br
patrickmelo13@gmail.com
washington_605@hotmail.com
gibran.cas@gmail.com

Abstract. *This research intends to study the movement of a rotating blunt body at sea level along its trajectory, focusing specifically on its axial rotation. This study is significant as it can be applied in analyzing external ballistics and trajectory analysis of small self-stabilizing rockets and bullets. The numerical analysis was based on the solution of Navier-Stokes equations per two approaches: bi- and three-dimensional simulation of compressible flow. In the 2D model, the tools utilized were the classical axisymmetric and swirling models. The 3D simulation confirmed the 2D model and analyzed lateral forces due to side wind. The numerical calculation performed through trajectory equations presents a model that can provide both direct and reverse calculations for trajectory recovery. Furthermore, finally, an experimental study was conducted to validate numerical simulations. It is based on measuring trajectory parameters, including the initial body angle, final angle, average velocity, and wind velocity. As a result of this research, a versatile trajectory model was built and validated.*

Keywords: *Blunt body, Navier-Stokes Equation, 3D simulation, Trajectory recovery.*

1. INTRODUCTION

The study of blunt bodies has always intrigued aerodynamicists due to their shock wave simplicity and properties. The applicability of this type of geometry in areas such as forensics analysis and atmospheric reentry of objects, including capsules and interplanetary probes, has motivated more in-depth studies to predict its behavior more precisely, aiming for greater efficiency in projectile trajectory tracing.

Recognizing the importance of blunt bodies for the many fields of engineering, this paper tends to evaluate the trajectory of four rotating blunt bodies (Xu and Dong, 2022) at sea-level conditions for different Mach numbers through two alternatives: simulations performed in 2D and 3D based on Navier-Stokes equations and analytical calculations using Second Law of Newton. Finally, experimental tests will help to measure the angle of departure and arrival, trajectory time, and range, aiming to validate numerical and analytical results.

The primary motivation for making this study is to develop a simple and reliable computational methodology for trajectory recovery of subsonic and transonic blunt bodies (Deng *et al.*, 2020), with practical applications in mind. The research team embarked on this project in response to a request from the criminalistic department of the civil police of the Federal District. The authors divided their efforts into two parts to tackle the task at hand.

The first part focuses on trajectory analysis and recovery, where the available information includes the final velocity and body shape. The unknown parameters to be determined are the aerodynamic characteristics of the body, trajectory profile, and initial trajectory point. Simultaneously, the second part involves the aerodynamic analysis of blunt bodies to determine the aerodynamic coefficients necessary for further trajectory calculations. These two aspects will be developed in parallel and validated through experiments in the future.

Additionally, the current work has an essential application in predicting the descent trajectory of sounding rockets, a crucial analysis for the planning and testing rocket launches. Consequently, the tasks of trajectory modeling and aerodynamic studies can be developed independently and integrated into the final stages of the methodology.

The main goal of this research is to construct a calculation methodology, which entails specific tasks such as selecting an appropriate computational fluid dynamics (CFD) model for simulating small-sized blunt bodies. Alternative options to be analyzed include bidimensional axisymmetric compressible flow without swirling motion, 2D flow with swirling

motion, and three-dimensional compressible flow with body rotation. Another task involves searching for a trajectory simulation method that utilizes the results obtained from the CFD analysis as input for determining the aerodynamic properties of the body. Finally, this research aims to provide a comprehensive and practical solution for trajectory recovery and aerodynamic analysis of subsonic and transonic blunt bodies by addressing these particular tasks and developing an integrated methodology.

2. SIMULATION OF THE BLUNT BODIES

The current study focuses on subsonic and transonic flow regimes, typical for blunt bodies in free flight, corresponding to Mach number from 0.1 to 0.9. The main output required from the numerical simulations is the drag coefficient for different flight velocities $C_D = f(M)$. As known (Anderson, 2017), the primary source, around 90%, of drag for blunt bodies is pressure drag, and only nearly 10% is skin friction drag. However, calculating the boundary layer is essential for shock wave-body interaction problems (Ruban, 2017). For the simplicity of the computational problem, the flow was assumed to be stationary. Then, the drag coefficient table for various Mach numbers will be approximated by the spline function for implementation in the trajectory model.

First, the flow model adopted in this paper was based on Euler's equation system. However, after comparing the viscous flow model, it was verified that the inviscid values were considerably lower than the viscous values. Thus, it was concluded that due to the discrepancy in results between the two models, the effects of viscosity could not be neglected; therefore, the inviscid analysis was not considered satisfactory for the paper.

In the vast majority of flows, the effects of turbulence are significant and must be widely considered. To Kundu and Cohen (2002), the complexity is the impossibility of only analytically approaching turbulent flows. Therefore, it becomes indispensable to implement simulated turbulence models to solve complex problems.

The flow around the geometries shown in Figure 1 was simulated using the software Ansys® Fluent to find the drag coefficient as a function of the Mach Number. Four kinds of simulations for Geometry 4 (Figure 1) were made to decide the most appropriate simulation conditions: 2D inviscid flow, 2D viscous flow, 2D viscous flow with swirl, and 3D viscous flow with swirl. All the simulations were made using the axisymmetric k-ω SST model (Rollet-Miet *et al.*, 1999; Bardina *et al.*, 1997), taking into account compressibility effects.

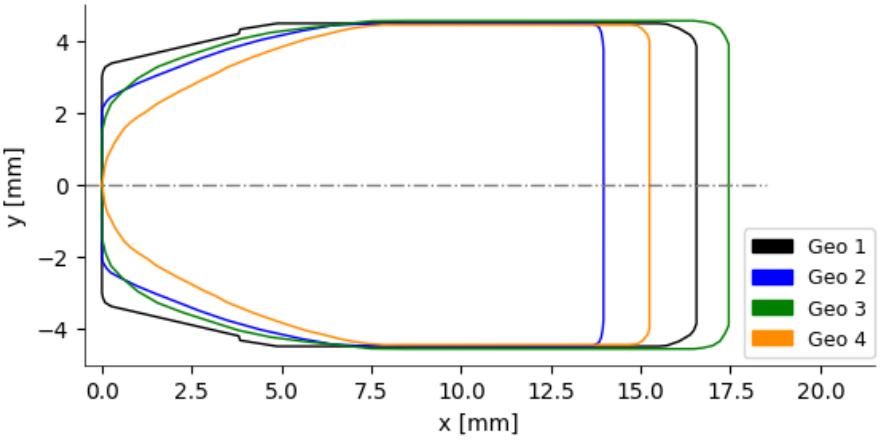

Figure 1: The blunt bodies' geometries.

The authors designed and implemented a computational domain with the primary objective of creating a structured mesh. Figure 2a shows a two-dimensional computational domain, while Figure 2b showcases a three-dimensional computational domain with labeled boundary conditions. The dimensions of the domain are directly related to the length of the blunt body (C), measuring $10C$ in the axial direction and $10C$ in the radial direction. A C-mesh comprising 280×75 computational cells was constructed to encompass the body adequately. Furthermore, an additional domain of 120×240 elements was incorporated into the near-wall zone.

To ensure an accurate representation of the boundary layer near the wall, a bias of 80.0 units was employed, compressing the mesh in the near-boundary layer zone. For the 3D simulation, the same mesh structure as the 2D model was utilized, extending the number of elements in the cross-section into the third dimension through a revolution of the 2D structure. In the angular direction of the 3D volume (Fig. 2b), the domain was divided into 60 equally spaced divisions.

A mesh sensitivity analysis was conducted, considering the maximum $y+$ criterion and the minimum value of the drag coefficient (C_D). The analysis revealed that the number of elements used in the 2D simulation, $55,277$, and the 3D simulation, $3,382,920$, were sufficient to achieve accurate results.

However, it is worth noting that due to the physical limitations of the current study and to ensure better readability, the findings and results obtained from this research will be published in subsequent papers. These future papers will provide

a more comprehensive analysis and discussion of the study, allowing for a more in-depth exploration of the topic.

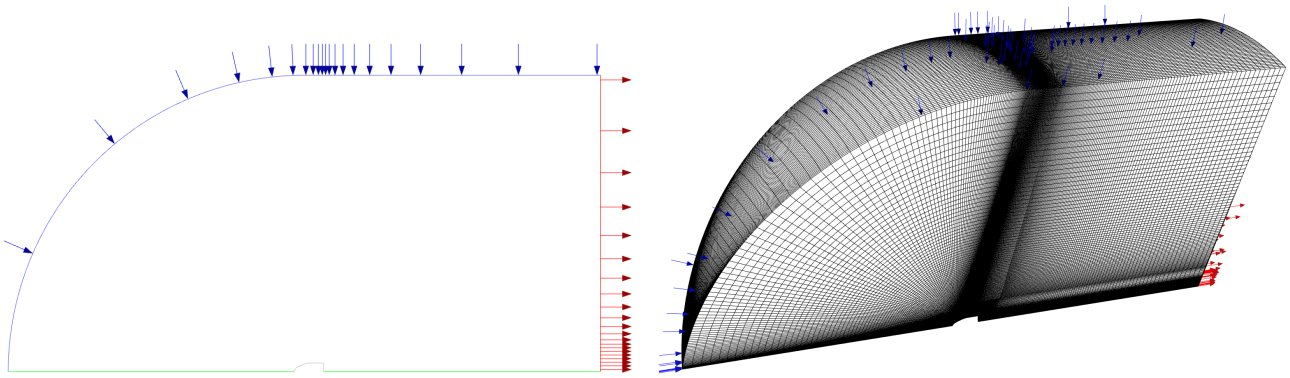

(a) 2D computational volume. (b) 2-3D volume and mesh.

Figure 2: Computational volumes for 2D and 3D analysis.

The boundary conditions were defined as follows. For the computational domain's inlet surface, referred to as the "far-field velocity," Riemann boundary conditions were applied. These conditions were set based on the flow Mach number, ranging from 0.1 to 0.9 with an increment of 0.1. A zero pressure gradient condition, named "pressure outlet", was imposed on the outlet boundary to represent the flow behavior at the domain's exit accurately.

For the wall boundaries, no-slip conditions were implemented. Additionally, a body axial rotation of 6 degrees relative to the free-stream Mach number was implemented to consider rotational effects on the flow.

The "symmetry" boundary condition, which reflects the velocity, was applied to the symmetry planes in the 3D simulation. This condition ensures that the velocity components normal to the symmetry plane are mirrored, simulating the effect of symmetry in the flow.

In the case of the 2D axisymmetric simulation, the "axis" boundary condition was set at the symmetry axis, specifically at $y = 0$. This condition preserves the symmetry of the flow by maintaining a zero velocity component in the axial direction at the axis of symmetry.

2.1 Method of solution

The methodology used to solve the averaged Navier-Stokes equations will be comprehensively presented in the final version of the manuscript. This detailed description will outline the specific numerical techniques, algorithms, and computational methods employed to solve the equations and obtain the desired results. By providing a clear and thorough explanation of the solution methodology, the manuscript will ensure transparency and reproducibility, allowing readers to understand and replicate the computational approach used in the study.

The convergence of the solution was determined using the following approach. For subsonic flows up to Mach number 0.6, the residual convergence criteria were set to 10^{-4} for all flow parameters. This ensured that the solution reached a sufficiently accurate level.

However, for flows with Mach numbers greater than 0.6, where transonic effects come into play, the residuals alone were not considered the sole indicator of convergence. Instead, the authors focused on analyzing the behavior of the drag coefficient (C_D). They observed that, after many simulation steps, C_D oscillated around an average value. This oscillation was attributed to the periodic displacement of the shock wave structure.

Upon detecting this oscillatory behavior in C_D, the average value of C_D was calculated and used as the final simulation result. This approach took into account the influence of the shock wave structure and provided a more accurate representation of the flow behavior in the transonic regime.

2.2 Bidimensional Simulation

The authors of this paper will present Figure 3, which displays the drag coefficient values obtained for nine distinct Mach numbers across four different geometries. These results will provide insights into the variations of the drag coefficient with respect to different flow conditions and geometries.

Additionally, the section includes a comprehensive analysis of the flow structure based on the two-dimensional simulation. A comparative study between the two-dimensional simulation and the corresponding three-dimensional results was developed, allowing a detailed examination of the flow characteristics and their variations in different dimensions.

The data points obtained for the C_D as a function of the Mach number in Figure 3 were interpolated using a cubic spline interpolation method.

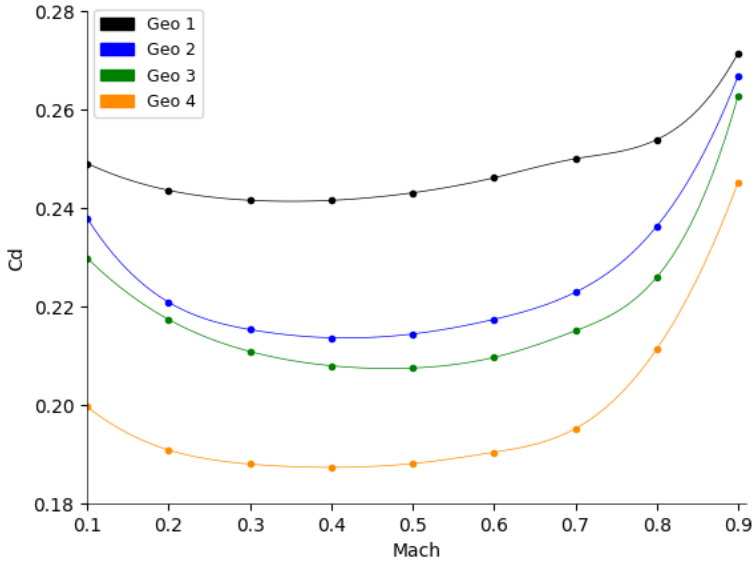

Figure 3: The blunt bodies' drag coefficients.

2.3 Tridimensional Simulation

In this section, notable distinctions between transonic flows are observed, particularly regarding the formation of shock waves around a blunt body and their interaction with the boundary layer. To provide a visual representation of the flow behavior, flow visualization techniques were employed at a specific moment when the drag coefficient reached its average level.

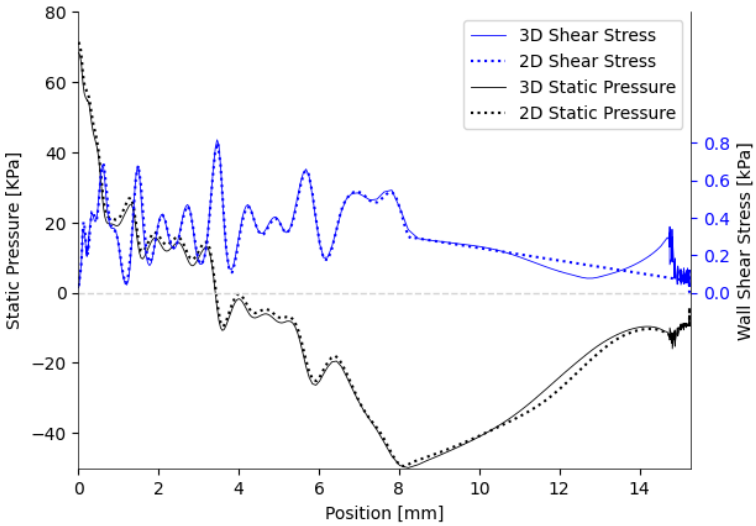

Figure 4: Pressure and shear stress distributions on the wall of the blunt body for $\mathrm{M} = 0.9$ in bi- and three-dimensional simulations.

The simulations revealed that the difference in drag coefficient between the two-dimensional and three-dimensional simulations was found to be less than 4 percent. This observation justifies the adoption of the dimensional flow analysis, which yields high-quality results. These results can be effectively utilized for subsequent trajectory analysis and related investigations. Figures 4 and 5 also show more similarities between the 2D and 3D simulations, namely, the distribution of static pressure and shear stress on the surface of the blunt body for $\mathrm{M} = 0.9$ and the pressure distribution around the body, respectively.

One significant advantage of conducting two-dimensional simulations compared to three-dimensional simulations is the considerable time savings achieved. The 2D simulations demonstrated a time savings of nearly 60 times compared to their 3D counterparts. This accelerated computational process facilitates the rapid analysis of new blunt body geometries, as well as the efficient implementation of drag coefficient calculations in trajectory analysis.

The reduced computational time associated with 2D simulations enables researchers to explore a broader range of

blunt body designs and evaluate their performance more quickly. Moreover, the obtained drag coefficient values can be readily incorporated into trajectory analysis, allowing for faster assessment and optimization of the body's aerodynamic behavior in various flight scenarios.

Overall, the time savings achieved by employing 2D simulations not only expedite the evaluation of new geometries but also streamline the integration of drag coefficient data into trajectory analysis, ultimately enhancing the efficiency of the overall research process.

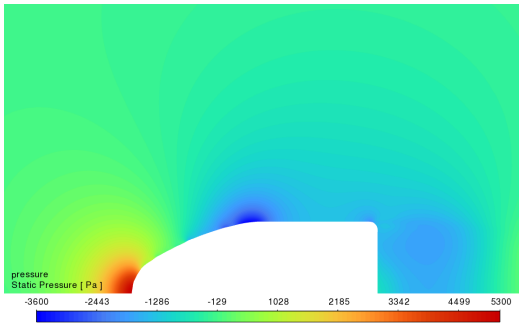

(a) 2D subsonic (M = 0.3).

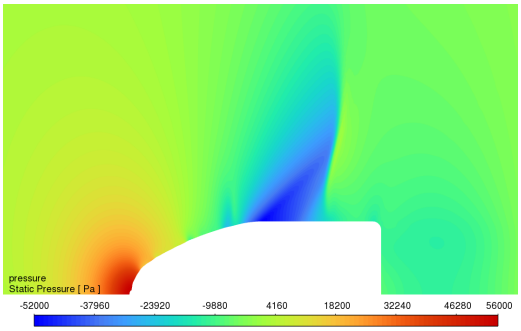

(b) 2D transonic (M = 0.9).

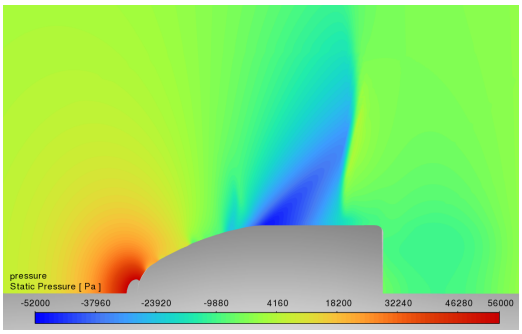

(c) 3D transonic (M = 0.9).

Figure 5: Pressure distribution around a blunt body.

3. TRAJECTORY MODELLING

The trajectory model was constructed according to Figure 6.

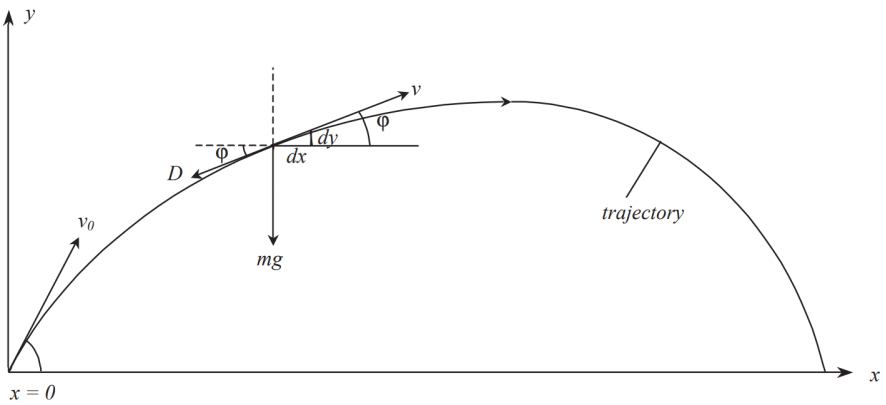

Figure 6: Trajectory schematics for a blunt body geometry (modified from Akçay (2004)).

By applying Newton's Second Law in the x and y direction, we obtain the system of ordinary differential equations (ODE) given by (1), where m is the mass of the studied geometries, D is the drag force, φ is the angle the trajectory makes with the x positive axis and g is the gravitational acceleration.

$$mx''(t) = -D\cos(\varphi) \qquad \text{and} \qquad my''(t) = -D\sin(\varphi) - gm \tag{1}$$

The drag force D can be written as in equation (2), where the density $\rho = 1.225\text{kg/m}^3$ and the cross-sectional area

$S = 6.36 \times 10^{-5}\text{m}^2$ are constants.

$$D = \frac{C_D \rho v^2}{2S} \tag{2}$$

In equation 2, the drag coefficient C_D is a function of the Mach number $M = v/a$, where the speed of sound a is considered constant and equal to 340.9m/s for standard sea-level conditions. The value of C_D is approximated by a fifth-order polynomial regression fit, as shown in equation (3), in which the coefficients a_i are obtained by fitting the simulated values for the drag coefficient into the polynomial.

$$C_D(M) = a_5 M^5 + a_4 M^4 + a_3 M^3 + a_2 M^2 + a_1 M + a_0 \tag{3}$$

The velocity v and angle φ can also be written in terms of the derivatives of the x and y position in respect to the time t.

$$v = \sqrt{(x')^2 + (y')^2} \tag{4}$$

$$\varphi = \tan^{-1}\left(\frac{y'}{x'}\right) \tag{5}$$

Finally, the substitution of equations (2), (4) and (5) into equation (1) leads to the following ODE's (6)

$$x'' = -\frac{C_D S \rho((x')^2 + (y')^2)}{2m\sqrt{1 + (y'/x')^2}} \qquad \text{and} \qquad y'' = -\frac{C_D S \rho((x')^2 + (y')^2)}{2m\sqrt{1 + (y'/x')^2}} - g \tag{6}$$

4. TRAJECTORY AND DEPARTURE ANGLE

With the help of Sympy, Python's symbolic math package, the polynomial equation (3) for the C_D as a function of the velocity v (equation (4)) is inserted into the ODE's (6). The result was then numerically integrated with the help of Python's Scipy "initial value problem" package, so that the trajectory, for a given geometry and initial velocity (departure velocity) v_0, would be a function of the initial angle (departure angle) φ_0 only. Figure 7 shows an example of calculated trajectories for the Geometry 1 for six different initial angles φ_0.

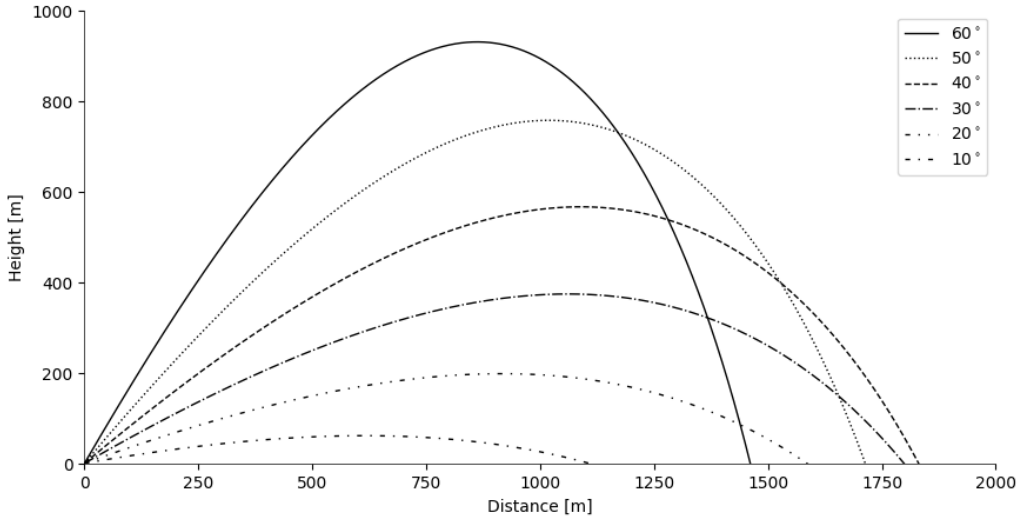

Figure 7: Calculated trajectories for Geometry 1.

It is also of the interest of the authors of this paper to understand the trajectory traced by the geometries given its final conditions. More specifically, given the final angle φ_f in which the geometry reached $y = 0$, how much distance Δx was covered by the geometry. These values are plotted in Figure 8 for the four studied geometries.

5. EXPERIMENTAL ANALYSIS

With the support of Civil Police of Sudoeste, some field tests were conducted in order to validate the numerical calculation. At one of its facilities, it was assembled a device that would let off one of the studied geometries bodies with $0°$ departure angle that would travel 22.58m before hitting a stopping device. With the help of a chronograph and laser sights, two measurements were made, the initial velocity v_0 of the launched body and its final drop height Δy.

After 18 launches of one of the studied geometries bodies, we observed a mean decrease in height of 35.78mm, while our calculations expected a decrease of 35.07mm, less than 2% in difference. Even though the results are close to the expected values, showing a good precision, the tests lack accuracy. Further testing proved necessary, highly increasing the number of launches, with more stable launching apparatus and better suited measurement equipment.

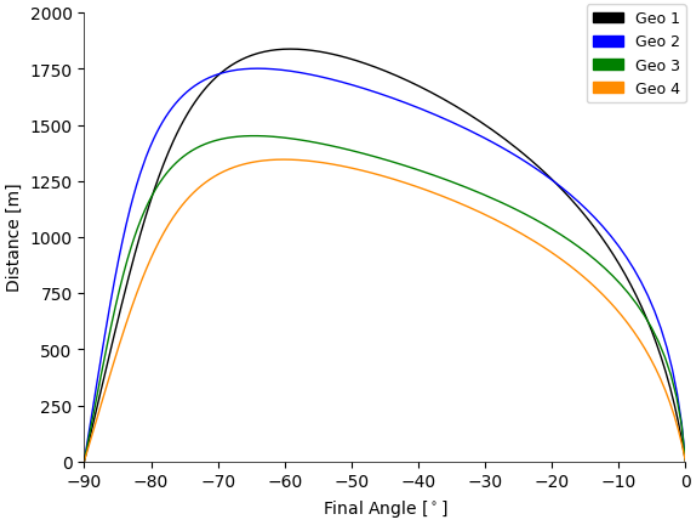

Figure 8: Distance Δx as a function of final angle φ_f.

6. CONCLUSIONS

In conclusion, this study addressed two distinct aspects of the problem at hand. Firstly, trajectory analysis necessitates a dependable drag coefficient, which can be acquired through either experimental or numerical investigations. Secondly, a numerical methodology was developed to simulate blunt bodies in subsonic and transonic regimes, enabling the accurate determination of their respective drag coefficients.

The comparison between bi-dimensional and three-dimensional simulations revealed a negligible deviation, affirming the suitability of two-dimensional simulations for further analysis, considering the substantial time savings associated with them.

Crucially, reliable drag coefficient values were successfully obtained for four distinct blunt body geometries using the numerical methodology. These values lay the groundwork for trajectory analysis and will aid in optimizing the aerodynamic performance of the bodies under various flight conditions.

In addition, experimental analysis is planned to validate the numerical results, and these findings will be presented in forthcoming studies. By combining experimental and numerical insights, a comprehensive understanding of the flow behavior and drag characteristics of the blunt bodies will be attained, contributing to advancing aerodynamic research and related applications.

7. ACKNOWLEDGEMENTS

We want to thank the Civil Police of Sudoeste for giving us the opportunity to test our project in their test fields and the Chemical Propulsion Laboratory and Capital Rocket Team for providing infrastructure, equipment, and software for numerical analysis. And finally, the University of Brasilia for believing in its students and prioritizing education.

8. REFERENCES

Akçay, M., 2004. "Development of universal flight trajectory calculation method for unguided projectiles".

Anderson, 2017. *Fundamentals of Aerodynamics*. Aeronautical and Aerospace Engineering. Mc Graw Hill Education, 6th edition.

Bardina, J.E., Huang, P.G. and Coakley, T.J., 1997. "Turbulence modeling validation, testing, and development". Technical report, Moffett Field, California.

Deng, Z.L., Shen, Q., Cheng, J.S. and Wang, H.Y., 2020. "Trajectory estimation method of spinning projectile without velocity input". *Measurement*. doi:10.1016/j.measurement.2020.107831.

Rollet-Miet, P., Ferziger, J. and Laurence, D., 1999. "Les and rans of turbulent flow in tube bundles". *International Journal of Heat and Fluid Flow 20(3): 241-254.* doi:10.1016/S0142-727X(99)00006-5.

Ruban, A.I., 2017. *Fluid Dynamics: Part 3 Boundary Layers*. Oxford University Press. ISBN 9780199681754. doi: 10.1093/oso/9780199681754.001.0001. URL `https://doi.org/10.1093/oso/9780199681754.001.0001`.

Xu, Y. and Dong, F., 2022. "Ballistic and aerodynamic characteristics simulation for trajectory correction projectile". *Mechanika*. doi:10.5755/j02.mech.31431.

9. RESPONSIBILITY NOTICE

The authors are the only ones responsible for the printed material included in this paper.